SHP2 is overexpressed and inhibits pSTAT1-mediated APM component expression, T cell attracting chemokine secretion, and CTL recognition in head and neck cancer cells

Michael S. Leibowitz[*], **Raghvendra M. Srivastava**[†], **Pedro A. Andrade Filho**[†], **Ann Marie Egloff**[†], **Lin Wang**[‡], **Raja R. Seethala**[‡], **Soldano Ferrone**[*,§], and **Robert L. Ferris**[*,†,¶]

[*]Department of Immunology, University of Pittsburgh, Pittsburgh, PA

[†]Department of Otolaryngology, University of Pittsburgh, Pittsburgh, PA

[‡]Department of Pathology, University of Pittsburgh Cancer Institute, Pittsburgh, PA

[§]Department of Surgery, University of Pittsburgh Cancer Institute, Pittsburgh, PA

[¶]Cancer Immunology Program, University of Pittsburgh Cancer Institute, Pittsburgh, PA

Abstract

Purpose—Human leukocyte antigen (HLA) class I antigen processing machinery (APM) component downregulation permits escape of malignant cells from recognition by cytotoxic T lymphocytes (CTL) and correlates with poor prognosis in patients with head and neck cancer (HNC). Activated STAT1 (pSTAT1) is necessary for APM component expression in HNC cells. We investigated whether an overexpressed phosphatase was responsible for basal suppression of pSTAT1 and subsequent APM component-mediated immune escape in HNC cells.

Experimental Design—Immunohistochemical staining and RT-PCR of paired HNC tumors was performed for the phosphatases src homology domain-containing phosphatase (SHP)-1 and SHP2. Depletion of phosphatase activity in HNC and STAT1$^{-/-}$ tumor cells was achieved by siRNA knockdown. HLA class I restricted, tumor antigen specific CTL were used in IFN-γ ELISPOT assays against HNC cells. Chemokine secretion was measured after SHP2 depletion in HNC cells.

Results—SHP2 but not SHP1 was significantly upregulated in HNC tissues. In HNC cells, SHP2 depletion significantly upregulated expression of pSTAT1 and HLA class I APM components. Overexpression of SHP2 in nonmalignant keratinocytes inhibited IFN-γ-mediated STAT1 phosphorylation and SHP2 depletion in STAT1$^{-/-}$ tumor cells did not significantly induce IFN-γ-mediated APM component expression, verifying STAT1 dependence of SHP2 activity. SHP2 depletion induced recognition of HNC cells by HLA class I restricted CTL and secretion of inflammatory, T cell attracting chemokines, RANTES and IP10.

To whom correspondence should be addressed: Robert L. Ferris, MD, PhD, Hillman Cancer Center Research Pavilion, 5117 Centre Avenue, Room 2.26b, Pittsburgh, PA USA 15213-1863, Phone: 412-623-0327, Fax: 412-623-4840, ferrisrl@upmc.edu.
There are no conflicts of interest.

Conclusion—These findings suggest for the first time an important role for SHP2 in APM-mediated escape of HNC cells from CTL recognition. Targeting SHP2 could enhance T cell-based cancer immunotherapy.

Keywords

SHP2; STAT1; immune escape; APM component; HNC

Introduction

In the majority of cases, T cell-based cancer immunotherapies have yielded detectable immune responses in the absence of appreciable clinical activity (1). Several immune escape mechanisms have been identified in head and neck squamous cell carcinoma (HNC) patients. At the effector phase level they include recruitment of regulatory T cells and myeloid derived suppressor cells into the tumor microenvironment (2) and reduction of absolute T lymphocyte counts (3). At the target cell level, a major mechanism is represented by downregulation of antigen processing machinery components; this abnormality leads to poor tumor antigen (TA) processing and presentation (4-7). As a result, HNC cells are poorly recognized by cognate HLA class I antigen restricted, tumor antigen (TA)-specific cytotoxic T lymphocytes (CTL) (4, 7, 8). Interestingly, antigen processing machinery (APM) component downregulation correlates with poor prognosis in patients with HNC (6), demonstrating that this escape mechanism is clinically significant. The molecular mechanism for this poor TA presentation has been characterized only to a limited extent.

Previous work has demonstrated that treatment of HNC cells with interferon gamma (IFN-γ) upregulates APM components and restores TA-specific CTL lysis *in vitro* (4). In prior studies, we have shown that APM expression and T cell recognition require IFN-γ-STAT1 pathway activation (4, 9). The low basal pSTAT1 levels in HNC cells led us to investigate regulatory mechanisms that disrupt STAT1 activation, APM component expression, T cell recruitment and subsequent recognition of HNC cells.

Since we have recently found that HNC cells express basal total (unphosphorylated) STAT1, but not activated pSTAT1 (9), we hypothesized that a negative regulator of STAT1 phosphorylation might be responsible for low APM component expression and CTL escape in HNC cells. Src homology-2 domain-containing phosphatase (SHP)-2 has been suggested as a negative regulator of the JAK-STAT signal transduction pathway (10, 11) but it has not been implicated in tumor immune escape. Furthermore, SHP2 overexpression and/or hyperactivity have been demonstrated in leukemia, breast, and bladder cancers (12, 13). Thus, we investigated whether overexpression of SHP2 might provide a novel mechanism for CTL escape through dephosphorylation of pSTAT1 in cancer cells, reducing expression of HLA class I APM components as well as pro-inflammatory cytokines and chemokines.

Materials and Methods

Cell lines

The HLA-A*0201[+] HNC cell lines, PCI-13 and SCC-90 (14) and HLA-A*0201[-] cell lines, SCC-4 and PCI-15B were characterized and described previously (15). All tumor cell lines were cultured in DMEM (Sigma-Aldrich Inc, St. Louis, MO) supplemented with 10% FBS (Mediatech, Herndon, VA), 2% L-glutamine, and 1% penicillin/streptomycin (Life Technologies, Grands Island, NY). Keratinocytes were described previously (16) and grown in keratinocyte serum-free medium (Keratinocyte-SFM; Life Technologies) supplemented with bovine pituitary extract. Parental 2fTGH (STAT1$^{+/+}$) and U3A (STAT1$^{-/-}$) fibrosarcoma cells (a kind gift from Dr. George Stark, Cleveland Clinic Foundation,

Cleveland, Ohio) were cultured in IMDM (Life Technologies) supplemented with 10% FBS (Mediatech, Herndon, VA), 2% L-glutamine, and 1% penicillin/streptomycin (Life Technologies).

Cytokines

Human IFN-γ was purchased from InterMune (Brisbane, CA). IFN-γ concetration in cell culture supernatants was determined by human IFN-γ ELISA kit (R&D systems) according to manufacturer's instructions. In the experimental conditions used, 100 U/ml of recombinant IFN-γ equated to 1464 pg/ml using this ELISA kit.

Antibodies

Anti-HLA-A, B, C mAb (W6/32) (EBiosciences, San Diego, CA) and anti-HLA-DR (L243) mAb (Biolegend, San Diego, Ca) were used in ELISPOT assays. LMP2-specific mAb SY-1 (17), TAP1-specific mAb NOB-1, TAP2-specific mAb NOB-2, and calreticulin-specific mAb TO-11, were developed and characterized as described (17, 18). FITC conjugated IgG anti-mouse mAb (Life Technologies) was used as a secondary antibody for APM components. The intracellular pSTAT staining was performed using PE conjugated irrelevant IgG2a mAb isotype control, PE conjugated phosphorylated tyrosine 701 STAT1 mAb (pSTAT1 Tyr701). Alexa Fluor 647-conjugated total STAT1 mAb, FITC conjugated phosphorylated serine 727 STAT1 mAb (pSTAT1 Ser 727), PE conjugated pSTAT1 Tyr 701, pSTAT3 Tyr705 mAb, and FITC conjugated phosphorylated serine 727 STAT3 mAb (pSTAT3 Ser 727) were purchased from BD Biosciences (San Jose, CA),. Anti-pSTAT1 Tyr701 mAb (Cell Signaling Tech, Danvers, MA), anti-total STAT1 (C-24) polyclonal (pAb) (Santa Cruz Biotech, Santa Cruz, CA), anti-β-actin mAb (Sigma-Aldrich Inc), anti-rabbit IgG-HRP (Promega, Madison, WI), anti-mouse IgG-HRP (Biorad, Hercules, CA), anti-phosphorylated JAK-1 (Tyr1022/1023) mAb, anti-phosphorylated JAK-2 (Tyr 1007/1008) mAb (Cell signaling Tech, Danvers, MA), anti-total JAK-1 mAb, anti-total JAK-2 mAb (Santa Cruz Biotech) were used in immunoblot blot analyses.

Immunohistochemistry

Protein levels were evaluated by immunohistochemical (IHC) staining of tumor and adjacent mucosal specimens arrayed in a previously described tissue microarray (TMA) (19). For the studies presented here, the maximum number of evaluable tumor specimens was 46, 16 of these tumors had arrayed adjacent mucosal tissues available for analysis. Tissue microarray quality assessment and morphologic confirmation of tumor or normal histology was performed using one H&E-stained slide for every ten tissue sections.

Arrayed tissues were IHC stained for SHP1 and SHP2 and tissue levels were evaluated semi-quantitatively. Prior to incubation with anti-SHP1 (Santa Cruz Biotech) or anti-SHP2 (Santa Cruz Biotech) antibodies for 60 minutes at room temperature, antigen retrieval was performed using citrate pH 6 buffer (Dako) followed by incubation with a 3% hydrogen peroxide solution for 5 min at room temperature (RT). The tissue specimens were then blocked with calf serum block (Life Technologies) for 10 minutes at room temperature. SHP1 staining was developed using Dako Dual Envision+ for 30 minutes at room temperature followed by incubation with Substrate Chromagen for 5 minutes at room temperature. Slides were counterstained with Harris Hematoxylin, and cytoplasmic and nuclear staining intensity (0 – 3) and percent of tumor cells to the nearest 5% were determined separately by a head and neck cancer pathologist. An IHC score was derived from the product of the intensity and percentage of tumor stained, and IHC scores for each core of a specimen were averaged.

Quantitative Real-Time RT-PCR

Total RNA from tumor samples and normal mucosa was extracted using Trizol reagent (Invitrogen) and purified using RNA cleanup (Qiagen), followed by DNase digestion (Ambion) according to manufacturer's instructions. The concentration and purity of RNA was determined by measuring absorbance at 260 and 280 nm. RNA was used for first strand cDNA synthesis using random hexamers and MuLV reverse transcriptase (Applied Biosystems, Foster City, CA) according to manufacturer's instructions. PCR probes for SHP2 (Hs00743983_s1) and β-actin (Hs99999903_m1) were purchased from Applied Biosystem for TaqMan® Gene Expression Assay. Real-time PCR cycling was performed (7700 Real-Time PCR System; Applied Biosystems, Carlsbad, CA) under the following conditions: denaturation at 95°C for 10s, annealing at 60°C for 15 s, and extension at 72°C for 30 s. An initial denaturation step at 95°C for 5 min and a final extension step at 72°C for 10 min were also included. PCR was performed for 40 cycles. β-Actin was amplified as an internal control. All of the experiments were performed in duplicates. Relative expression of the SHP2 gene to endogenous control gene (β-actin) was calculated using the ΔC_T method: relative expression $= 2^{-\Delta CT}$, where $\Delta C_T = C_{T\,(shp2)} - C_{T\,(\beta\text{-actin})}$.

Immunoblot Analysis

Cells were lysed in 10 mM Tris HCl, 5 mM EDTA, 50 mM NaCl, 30 mM $Na_2P_2O_7$, 50 mM NaF, 1 mM $NaVO_4$, 1% Triton X-100, 1 mM PMSF and vortexed for at least 1 hour at 4°C, sonicated for 6 seconds at 20% of the maximum potency (Cole Parmer Instrument, Verona Hills, IL) and centrifuged at 4°C, 16,100 g for 15 minutes. The supernatant protein was normalized and 40-60 μg of protein were size fractionated through a 4-12% SDS-PAGE gel (Lonza, Rockand, ME), transferred to a PVDF membrane (Millipore, Billerica, MA) and immunoblotted with the indicated antibodies.

Intracellular flow cytometry for APM component, pSTAT1 and total STAT1 expression

Briefly, the cells were fixed using 1.5% paraformaldehyde for 10 minutes at room temperature (RT) and permeabilized with 100% methanol for at least 24 hours at −20°C. Cells were then washed in 2% FCS/PBS (FACS buffer), and stained with either a PE conjugated primary STAT-specific mAb or sequentially by incubation with an unconjugated primary APM component-specific mAb and then with a FITC conjugated anti-mouse secondary mAb. Both incubations were for 30 minutes at RT. FACS analysis was performed on the same day as staining. Isotype control antibody staining was set at a mean fluorescence intensity (MFI) of 5 on an EPICS XL cytometer (Beckman Coulter, Brea, CA) or subtracted from each condition and cell line tested. A minimum of 10,000 cells were collected per test. Analyses were performed using EXPO32 ADC software (Beckman Coulter). pSTAT1, pSTAT3 and APM component expression was determined based on MFI and was expressed as a mean + SEM of the results obtained in at least three independent experiments.

Transfection of cells with small interfering RNA (siRNA)

HNC cell lines were transfected at 30-40% confluence with SHP1, SHP2 or a non-targeting siRNA control (Ambion, Austin, Tx), Lipofectamine RNAi max (Life Technologies), and Optimem I (Life Technologies) according to the Lipofectamine RNAi max instructions.

SHP1: 5′-GGUGACCCAUAUUCGGAUCTT′ (s) and 5′-GAUCCGAAUAUGGGUCACCTG-3′ (as)

SHP2: 5′-GGAGAACGGUUUGAUUCUUTT-3′ (s) and 5′-AAGAAUCAAACCGUUCUCCTC-3′ (as)

Non-targeting: 5′-AGUACAGCAAACGAUACGGtt-3′ (s) and 5′-CCGUAUCGUUUGCUGUACUtt-3′ (as)

SHP2 Plasmids

Keratinocytes were transfected at 80-90% confluence with wild type SHP2 (pcDNA3.1-myc-6xHis-SHP2) or mutant SHP2 (C4593) plasmid constructs (10μg/ml) (a kind gift from Dr. Gibbes Johnson, FDA). Lipofectamine 2000 reagent (Life Technologies) was used at a 1:2 dilution in Optimem I (Life Technologies) according to the Lipofectamine 2000 instructions.

ELISPOT Assay

ELISPOT assays were performed as described (20). Briefly, multiscreen$_{HTS}$-HA filter plates (Millipore) were coated with anti-human IFN-γ mAb 1-D1K (Mabtech, Mariemont, OH) (10 μg/mL in PBS) overnight at 4°C. Plates were washed with PBS and then blocked for 1 h at 37°C with DMEM supplemented with 10% human serum. EGFR$_{853-861}$ (20) and p53$_{65-73}$ (21, 22) specific CTL were added to wells in triplicate (5×10^4) and then HNC cells (5×10^4). Following an 18-24 hour incubation at 37°C, plates were washed with PBS/0.05% Tween 20 (PBS-T), and incubated with biotinylated anti-IFN-γ mAb (Mabtech) (2 μg/ml) for 4 hours at 37°C. Plates were washed with PBS-T avidin-peroxidase complex (Vector laboratories, Burlingame, CA) for 1 hour at RT then peroxidase staining was performed with 3,3,5′-tetramethylbenzidine (Vector Laboratories) for 4 minutes. Spots were enumerated in triplicate wells as a mean +/− standard error using computer-assisted video image analysis software (Cellular Technology Ltd., Shaker Heights, OH). HLA class I restricted recognition of the target cells by CTL was assessed by using the anti-HLA class I-specific mAb W6/32 (10 μg/ml) and the specificity of the inhibition was assessed using the HLA-DR-specific mAb L243 (10 μg/ml).

Chemokine expression assay

HNC cells were assayed for expression of various cytokines and chemokines using a human cytokine 30-plex panel (Life Technologies) as previously described (23), 48 hours after siRNA knockdown of SHP2 or irrelevant target.

Statistical Analysis

Data are expressed as a mean + standard error of the results obtained in at least three independent experiments. A two-tailed t-test was used to calculate whether observed differences were statistically significant, defined as $p < 0.05$. The signed rank test was used to evaluate differences in SHP1 and SHP2 levels between paired tumor and adjacent mucosal tissues and statistically significance was defined as $p < 0.05$.

Results

SHP2 but not SHP1 is overexpressed in HNC tissues

Previous work demonstrated that pSTAT1 is required for APM component expression in HNC cells (9, 24), and that the STAT1 agonist, IFN-γ, induced APM component upregulation and CTL recognition (4). Interestingly, we found that basal levels of pSTAT1 are undetectable in HNC cells, despite abundant expression of total STAT1 protein (9). To identify a mechanism for this phenotype, we tested whether a protein tyrosine phosphatase might be responsible for the dephosphorylation of activated STAT1. First, a panel of HNC cells, PCI-13, SCC-90, SCC-4, and PCI-15B, were treated with a broad phosphatase inhibitor, sodium orthovandate (SOV). After 24 hours of treatment with SOV (100uM), pSTAT1 levels were found to be significantly upregulated in these cells by immunoblot

analysis (data not shown). These data indicated that protein tyrosine phosphatases may contribute to the basal dephosphorylation of STAT1 in HNC cells.

Both SHP1 (25, 26) and SHP2 (10) have been suggested to be negative regulators of STAT1 phosphorylation. To assess SHP1 and SHP2 expression in human HNC, IHC staining of a clinically annotated tissue microarray (TMA) cohort of HNC patients was performed on paired tumor and normal mucosa. Interestingly, IHC analysis revealed that SHP2 was significantly overexpressed in tumor cells compared to normal mucosa (Figure 1A; p=0.002, signed rank test). Moreover quantitative RT-PCR analysis also showed higher levels of SHP2 transcript in tumor samples compared to normal mucosa (Figure 1B; p<0.05). This difference is selective, since no significant difference in SHP1 expression was detected between tumor and normal mucosa (Supplementary Figure 1). Therefore, we investigated the role of overexpressed SHP2 in HNC cells.

SHP2 depletion upregulates pSTAT1, pJAK1/2 and total STAT1 in HNC cells

Using siRNA (100nM, 48h), we obtained about 70% knockdown of SHP2 protein in PCI-13 (Figure 2A) and SCC-90 cells (Figure 2G). SHP2 knockdown significantly upregulated pSTAT1 tyrosine (Tyr) 701 in PCI-13 (Figures 2B & 2E p<0.002, two-tailed t-test) and SCC-90 cells (2H & 2K p<0.002, two-tailed t-test), total STAT1 in PCI-13 (Figures 2C & 2E) and SCC-90 cells (Figures 2I & 2K) but did not affect pSTAT1 serine (Ser) 727 in either PCI-13 (Figure 2D) or SCC-90 cells (Figure 2J). Also, SHP2 depletion did not affect expression of pSTAT3 Tyr 705 or pSTAT3 Ser 727 in PCI-13 cells (Supplementary Figures 2 A & B) or SCC90 cells (Supplementary Figures 2 C & D) compared to cells transfected with control siRNA. SHP2 depleted cells showed similar levels of STAT1 phosphorylation as compared to IFN-γ (100 U/ml, 10 min) treated cells (Figures 2B & 2E, and 2H & 2K). Interestingly, we also detected induction of pJAK1 (pTyr1022/1023) and pJAK2 (pTyr1007/1008) in SHP2 depleted PCI-13 (Figure 2F) and SCC-90 cells (Figure 2L) in comparison to control siRNA. IFN-γ treatment did not alter SHP2 levels under these conditions (data not shown).

To confirm that SHP1 was not involved in STAT1 activation, we investigated whether SHP1 depletion could upregulate pSTAT1 and APM component expression in HNC cells. Under conditions in which SHP1 siRNA (100nM, 48 h) achieved >70% knockdown of SHP1 protein compared to siRNA control (Supplementary Figures 3 A-B), we did not observe upregulation of pSTAT1 or APM components (Supplementary Figures 3 C-D). These data prompted us to focus on SHP2 activity as the primary negative regulator of STAT1 phosphorylation, APM expression, and CTL recognition of HNC cells.

Next, we investigated how STAT1 becomes activated after SHP2 depletion. We tested whether SHP2 depletion induces secretion of a STAT1 agonist cytokine. To explore this potential mechanism, HNC cells were treated with conditioned media (CM) from the same cell lines that were previously treated with IFN-γ (100 U/ml, 48h), or transfected with control or SHP2 siRNA (100nM, 48h). Interestingly, HNC cells treated with SHP2 siRNA CM induced STAT1 (Tyr) 701 phosphorylation (data not shown).

SHP2 depletion upregulates HLA class I APM component expression in HNC cells

Next, we investigated whether SHP2 depletion and subsequent enhancement of pSTAT1 led to an upregulation of HLA class I APM component expression in HNC cells. Indeed, SHP2 depletion by siRNA (100nM, 48h) induced significant upregulation of APM components in both PCI-13 and SCC-90 cells compared to control siRNA treated cells (Figures 3A-B; p<0.003, two-tailed t-test). STAT1 phosphorylation induced by SHP2 depletion did not upregulate all of the APM components, since no change was detected in the expression of

calreticulin, a non-IFN-γ-pSTAT1 inducible APM component (Figures 3A-B). IFN-γ (100 U/ml, 48h), a well characterized agonist of HLA class I APM component expression was used to compare relative APM component induction following siRNA transfections. In addition to upregulating APM components, SHP2 depletion by siRNA (100 nM, 48h) also significantly upregulated HLA class I molecule expression compared to control siRNA treated HNC cells (Figures 3C-D; $p < 0.02$, two-tailed t-test).

SHP2 regulates TAP1/2 expression in a STAT1-dependent fashion

We then examined whether transfection of SHP2 conferred a similar phenotype of APM component downregulation in non-malignant keratinocytes, and whether this effect was dependent on STAT1. Interestingly, cultured keratinocytes have significantly higher basal activated STAT1 and IFN-γ-induced pSTAT1 compared to HNC cell lines, PCI-13 and SCC-90 (data not shown). Furthermore, overexpression of wild type (WT) SHP2 in keratinocytes decreased both basal and IFN-γ-induced STAT1 phosphorylation compared to dominant negative, mutant SHP2 demonstrating that SHP2 overexpression suppressed STAT1 activation in epithelial cells (Figure 4A). In addition, IFN-γ-induced TAP1/2 expression in STAT1$^{+/+}$ fibrosarcoma cells were significantly increased after SHP2 depletion compared to both IFN-γ treatment alone and control siRNA, and this effect was abrogated in STAT1$^{-/-}$ fibrosarcoma cells (Figures 4B-C). These data verify that SHP2 mediates APM component upregulation through STAT1 activation, and supports the notion that SHP2 overexpresssion confers an "escape" phenotype of APM component downregulation in HNC cells.

SHP2 depletion induces HNC cell recognition by TA-specific CTL

The observation that SHP2 depletion significantly upregulated pSTAT1 and HLA class I APM components prompted our investigation into whether SHP2 depletion induced HNC cell recognition by CTL. Indeed, SHP2 depletion significantly increased PCI-13 and SCC-90 cell recognition by EGFR$_{853-861}$ and p53$_{65-73}$ specific CTL (Figures 5A-B; $p < 0.006$, two-tailed t-test). The recognition of HNC cells by TA-specific CTL is HLA class I restricted, since it was inhibited by the HLA-A, -B, -C specific mAb W6/32, but was not affected by HLA-DR specific mAb L243.

SHP2 depletion induces secretion of chemokines by HNC cells

To investigate downstream effects of SHP2 depletion and pSTAT1 activation in HNC cells, we performed multiplex ELISA assays (Luminex™) to measure the secretion of several cytokines and chemokines. Interestingly, significantly elevated levels of RANTES and IP10 were detected in the supernatants of HNC cells after SHP2 depletion by siRNA (100nM, 48h) compared to cells transfected with control siRNA (Figures 6A-B, $p < 0.008$, two-tailed t-test). Under similar conditions, MIG was not secreted by HNC cells after SHP-2 depletion whereas it was secreted after these cells were incubated with IFN-γ for 48h (Figures 6A-B). Notably, cytokines that induce STAT1 phosphorylation such as IFN-γ (Figures 6A-B) and IFN-α (data not shown) were not detected in the supernatants of HNC cells after SHP2 depletion despite expression of IFN receptors on HNC cells (9). Other cytokines and chemokines that were analyzed in this multiplex ELISA panel (IL-1β, IL-1RA, IL-2, IL-2R, IL-4, IL-5, IL-6, IL-7, IL-8, IL-10, IL-13, IL-15, IL-17, TNF-α, GM-CSF, G-CSF, Eotaxin, MCP-1, MIP-1α, MIP-1β, EGF, HGF, VEGF) were not detected (data not shown). Thus, SHP2 overexpression confers an immunosuppressive phenotype by reducing pSTAT1-mediated APM component expression and CTL recognition of HNC cells, and inhibits some proinflammatory, Th1 cell recruiting chemokines from the tumor microenvironment.

Discussion

Multiple mechanisms are utilized by tumor cells to escape recognition and elimination by the immune system. We describe a novel mechanism responsible for the phenotype of HLA class I APM component downregulation, namely suppression of STAT1 activation, leading to tumor cell escape from TA-specific CTL recognition and lysis, a widely observed phenomenon in many human cancers (4, 27, 28). These defects appear to be dependent on overexpression of SHP2, an SH2 domain-containing tyrosine phosphatase, which was found to be highly overexpressed *in vivo* in HNC tumor tissues (Figure 1), compared to surrounding normal epithelium. SHP2 is overexpressed and/or hyperactive in multiple malignancies (12, 13, 29-31), however few studies have investigated their impact on immune cell migration and recognition of tumor cells (32-35). To the best of our knowledge, this is the first report to demonstrate that SHP2 is significantly overexpressed in HNC tissue (Figure 1) with important biological consequences.

Our *in vitro* results demonstrate that SHP2 negatively regulates STAT1 phosphorylation in HNC cells. Expression of WT SHP2 decreased basal and induced pSTAT1 (Figures 4A), SHP2 depletion upregulated basal levels of pSTAT1 and total STAT1 (Figures 2B-C & E, 2H-I & K) and significantly augmented TAP1/2 expression by IFN-γ in STAT1 expressing cells but not in STAT1-deficient cells (Figures 4B-C). We did not observe differences in TAP1 expression after SHP2 depletion without pretreatment with IFNγ in STAT-1$^{+/+}$ and STAT-1$^{-/-}$ fibrosarcoma tumor cell lines, but details of the immune escape mechanisms in these unique fibrosarcoma cells is an interesting question of interest in our future studies. Fibrosarcoma tumor cells likely have other mechanisms that suppress APM expression beyond SHP2 activity and that the IFN-γ overcomes those other mechanisms.

Since pSTAT1 homodimers are important regulators of APM component genes (9, 24), our observation that pSTAT1 was upregulated in response to SHP2 (but not SHP1) depletion in HNC cells suggested that this effect could be sufficient to induce APM component expression, at a level comparable to that induced by IFN-γ treatment. Indeed, HLA class I APM component expression was upregulated after SHP2 depletion (Figure 3), and potentially induced HNC cell recognition by TA-specific CTL (Figure 5). Interestingly, knockdown of SHP2 also induced HNC cell secretion of proinflammatory, Th1 associated chemokines, RANTES and IP10 (Figure 6). These findings have potential clinical significance because SHP2 is upregulated in HNC tumors *in vivo*, suggesting that targeting SHP2 could increase the immunogenicity of HNC cells through upregulation of HLA class I APM components, while chemoattracting naïve and memory (CCR5$^+$) and Th1 (CXCR3$^+$) lymphocytes (36). This strategy could overcome a major limitation of T cell-based cancer immunotherapy, which is the reliance on the tumor cell to serve as a target for recognition by TA-specific T lymphocytes.

APM component downregulation as an escape mechanism (6, 7) of HNC cells from CTL recognition also correlates with poor prognosis (5, 6, 37, 38), and is observed in renal cell carcinoma (39), colorectal carcinoma (40), small cell lung carcinoma (41) and melanoma (42). Thus, investigation of the molecular regulators responsible for APM component defects is clinically important in HNC and the information derived from these studies may be generally applicable to a variety of other tumor types for which immunotherapy is currently being evaluated. Since mechanisms of immune escape utilized by tumor cells are complex and not mutually exclusive, we recognize that other suppressive effects on CTL, such as by Treg, may also cooperate to reduce elimination of tumor cells. The finding that SHP2 depletion enhances some chemoattracting Th1 type chemokines provides support for this approach to reverse the immunosuppressive phenotype in the microenvironment.

Previously, we demonstrated that IFN-γ treatment could restore CTL recognition and lysis of HNC cells (4), indicating that a regulatory, as opposed to a genetic mechanism was responsible for this escape phenotype. Furthermore, HNC cells were found to express abundant levels of total STAT1, but lack phosphorylated STAT1 (9). These finding suggested that a negative regulator of STAT1 phosphorylation might be responsible for the low pSTAT1 phenotype observed. Others have shown that protein tyrosine phosphatases can dephosphorylate and inactivate STAT1 (43); therefore we investigated whether protein tyrosine phosphatases might be responsible for low basal STAT1 phosphorylation in HNC cells. Indeed, treatment of a panel of HNC cells with a broad phosphatase inhibitor, sodium orthovandate (SOV), induced STAT1 phosphorylation to levels comparable or greater than those induced by IFN-γ treatment (data not shown). These data suggested that a phosphatase could contribute to the lack of pSTAT1 expression in HNC cells, maintaining a basal defect in the pro-apoptotic IFN-γ signal transduction pathway, and promoting immune escape. Further studies will analyze whether SHP2 overexpressed by HNC cells also contain activating mutations (31) or can be regulated by immunosuppressive cytokine(s), as suggested by others (31, 44).

The unexpected observation that SHP2 depletion not only reversed APM component downregulation and restored TA-specific CTL recognition of HNC cells (Figures 3 & 5), but also induced the secretion of RANTES and IP-10 by the tumor cells (Figure 6) has potential implications for T cell-based immunotherapy. RANTES strongly chemoattracts several immune cells, including eosinophils, basophils, mast cells, monocytes, NK cells, CTL, naïve CD4+ T cells, and memory T cells (45). RANTES also induces intratumoral infiltration of DCs, CD4+ T cells, CTLs, and NK cells (46) resulting in tumor growth inhibition *in vivo* (47). IP-10 has also been found to have antitumor activity by attracting CD4+ T cells, CTLs, and NK cells to the tumor microenvironment (48). Indeed, successful T cell-based immunotherapy has been linked to CXCR3 expression as a biomarker for active, tumor homing Th1 anti-tumor lymphocytes (36, 49).

Interestingly, MIG, another CXCR3 ligand, and MIP1-α (data not shown) and MIP1-β, CCR5 ligands, were not upregulated after SHP2 siRNA transfection, demonstrating specificity in chemokine secretion by the tumor cells after SHP2 depletion. Blockade of several STAT1 signaling receptors, such as IFN-γR, IFN-αR, and IL-10R, did not inhibit SHP2 siRNA-mediated STAT1 phosphorylation in HNC cells (data not shown). Further work is ongoing to elucidate the STAT1 agonist(s) secreted by HNC cells following SHP2 knockdown that are responsible for STAT1 phosphorylation and induction of these chemokines, as well as their cognate receptors.

In summary, SHP2 was investigated as a negative regulator of STAT1 phosphorylation and APM components in HNC cells. These novel data strongly indicate that SHP2 overexpression in HNC tumors *in vivo* may contribute to APM component downregulation and CTL evasion by HNC cells. Since SHP2 depletion increases the immunogenicity of HNC tumor cells, and may also induce recruitment of tumor antigen-specific immune effector cells to the tumor microenvironment. Future studies will investigate the effect of SHP2 inhibition on tumor cell growth *in vivo* using newly developed small molecule targeted agents as adjuvant efforts to enhance T cell-based immunotherapeutic approaches.

Supplementary Material

Refer to Web version on PubMed Central for supplementary material.

Acknowledgments

References

1. Koebel CM, Vermi W, Swann JB, Zerafa N, Rodig SJ, Old LJ, et al. Adaptive immunity maintains occult cancer in an equilibrium state. Nature. 2007; 450:903–907. [PubMed: 18026089]

2. Strauss L, Bergmann C, Gooding W, Johnson JT, Whiteside TL. The Frequency and Suppressor Function of CD4+CD25highFoxp3+ T Cells in the Circulation of Patients with Squamous Cell Carcinoma of the Head and Neck. Clin Cancer Res. 2007; 13:6301–6311. [PubMed: 17975141]

3. Kuss I, Hathaway B, Ferris RL, Gooding W, Whiteside TL. Decreased absolute counts of T lymphocyte subsets and their relation to disease in squamous cell carcinoma of the head and neck. Clin Cancer Res. 2004; 10:3755–3762. [PubMed: 15173082]

4. Lopez-Albaitero A, Nayak JV, Ogino T, Machandia A, Gooding W, DeLeo AB, et al. Role of antigen-processing machinery in the in vitro resistance of squamous cell carcinoma of the head and neck cells to recognition by CTL. J Immunol. 2006; 176:3402–3409. 2006. [PubMed: 16517708]

5. Ferris RL, Hunt JL, Ferrone S. Human leukocyte antigen (HLA) class I defects in head and neck cancer: molecular mechanisms and clinical significance. Immunol Res. 2005; 33:113–133. [PubMed: 16234579]

6. Meissner M, Reichert TE, Kunkel M, Gooding W, Whiteside TL, Ferrone S, et al. Defects in the human leukocyte antigen class I antigen processing machinery in head and neck squamous cell carcinoma: association with clinical outcome. Clin Cancer Res. 2005; 11:2552–2560. [PubMed: 15814633]

7. Ferris RL, Whiteside TL, Ferrone S. Immune escape associated with functional defects in antigen-processing machinery in head and neck cancer. Clin Cancer Res. 2006; 12:3890–3895. [PubMed: 16818683]

8. Lou Y, Vitalis TZ, Basha G, Cai B, Chen SS, Choi KB, et al. Restoration of the expression of transporters associated with antigen processing in lung carcinoma increases tumor-specific immune responses and survival. Cancer Res. 2005; 65:7926–7933. [PubMed: 16140964]

9. Leibowitz MS, Andrade Filho PA, Ferrone S, Ferris RL. Deficiency of activated STAT1 in head and neck cancer cells mediates TAP1-dependent escape from cytotoxic T lymphocytes. Cancer Immunol Immunother. 2011; 60:525–535. [PubMed: 21207025]

10. Shuai K, Liu B. Regulation of JAK-STAT signalling in the immune system. Nat Rev Immunol. 2003; 3:900–911. [PubMed: 14668806]

11. Baron M, Davignon JL. Inhibition of IFN-gamma-induced STAT1 tyrosine phosphorylation by human CMV is mediated by SHP2. J Immunol. 2008; 181:5530–5536. [PubMed: 18832710]

12. Tao XH, Shen JG, Pan WL, Dong YE, Meng Q, Honn KV, et al. Significance of SHP-1 and SHP-2 expression in human papillomavirus infected Condyloma acuminatum and cervical cancer. Pathol Oncol Res. 2008; 14:365–371. [PubMed: 18543080]

13. Su WP, Tu IH, Hu SW, Yeh HH, Shieh DB, Chen TY, et al. HER-2/neu raises SHP-2, stops IFN-gamma anti-proliferation in bladder cancer. Biochem Biophys Res Commun. 2007; 356:181–186. [PubMed: 17346677]

14. Ferris RL, Martinez I, Sirianni N, Wang J, Lopez-Albaitero A, Gollin SM, et al. Human papillomavirus-16 associated squamous cell carcinoma of the head and neck (SCCHN): a natural disease model provides insights into viral carcinogenesis. Eur J Cancer. 2005; 41:807–815. [PubMed: 15763658]

15. Heo DS, Snyderman C, Gollin SM, Pan S, Walker E, Deka R, et al. Biology, cytogenetics, and sensitivity to immunological effector cells of new head and neck squamous cell carcinoma lines. Cancer Res. 1989; 49:5167–5175. [PubMed: 2766286]

16. Piboonniyom SO, Duensing S, Swilling NW, Hasskarl J, Hinds PW, Munger K. Abrogation of the retinoblastoma tumor suppressor checkpoint during keratinocyte immortalization is not sufficient for induction of centrosome-mediated genomic instability. Cancer Res. 2003; 63:476–483. [PubMed: 12543805]

17. Bandoh N, Ogino T, Cho HS, Hur SY, Shen J, Wang X, et al. Development and characterization of human constitutive proteasome and immunoproteasome subunit-specific monoclonal antibodies. Tissue Antigens. 2005; 66:185–194. [PubMed: 16101829]

18. Ogino T, Wang X, Kato S, Miyokawa N, Harabuchi Y, Ferrone S. Endoplasmic reticulum chaperone-specific monoclonal antibodies for flow cytometry and immunohistochemical staining. Tissue Antigens. 2003; 62:385–393. [PubMed: 14617045]

19. Knowles LM, Stabile LP, Egloff AM, Rothstein ME, Thomas SM, Gubish CT, et al. HGF and c-Met participate in paracrine tumorigenic pathways in head and neck squamous cell cancer. Clin Cancer Res. 2009; 15:3740–3750. [PubMed: 19470725]

20. Andrade Filho PA, Lopez-Albaitero A, Gooding W, Ferris RL. Novel immunogenic HLA-A*0201-restricted epidermal growth factor receptor-specific T-cell epitope in head and neck cancer patients. J Immunother. 2010; 33:83–91. [PubMed: 19952953]

21. Andrade Filho PA, Ito D, Deleo AB, Ferris RL. CD8+ T cell recognition of polymorphic wild-type sequence p53(65-73) peptides in squamous cell carcinoma of the head and neck. Cancer Immunol Immunother. 2012; 59:1561–1568. [PubMed: 20577877]

22. Sirianni N, Ha PK, Oelke M, Califano J, Gooding W, Westra W, et al. Effect of human papillomavirus-16 infection on CD8+ T-cell recognition of a wild-type sequence p53264-272 peptide in patients with squamous cell carcinoma of the head and neck. Clin Cancer Res. 2004; 10:6929–6937. [PubMed: 15501971]

23. Linkov F, Lisovich A, Yurkovetsky Z, Marrangoni A, Velikokhatnaya L, Nolen B, et al. Early detection of head and neck cancer: development of a novel screening tool using multiplexed immunobead-based biomarker profiling. Cancer Epidemiol Biomarkers Prev. 2007; 16:102–107. [PubMed: 17220337]

24. Chatterjee-Kishore M, Kishore R, Hicklin DJ, Marincola FM, Ferrone S. Different requirements for signal transducer and activator of transcription 1alpha and interferon regulatory factor 1 in the regulation of low molecular mass polypeptide 2 and transporter associated with antigen processing 1 gene expression. J Biol Chem. 1998; 273:16177–16183. [PubMed: 9632673]

25. You M, Zhao Z. Positive effects of SH2 domain-containing tyrosine phosphatase SHP-1 on epidermal growth factor- and interferon-gamma-stimulated activation of STAT transcription factors in HeLa cells. J Biol Chem. 1997; 272:23376–23381. [PubMed: 9287352]

26. David M, Chen HE, Goelz S, Larner AC, Neel BG. Differential regulation of the alpha/beta interferon-stimulated Jak/Stat pathway by the SH2 domain-containing tyrosine phosphatase SHPTP1. Mol Cell Biol. 1995; 15:7050–7058. [PubMed: 8524272]

27. Marincola FM, Jaffee EM, Hicklin DJ, Ferrone S. Escape of human solid tumors from T-cell recognition: molecular mechanisms and functional significance. Adv Immunol. 2000; 74:181–273. [PubMed: 10605607]

28. Ferris RL, Whiteside TL, Ferrone S. Immune escape associated with functional defects in antigen-processing machinery in head and neck cancer. Clinical Cancer Research. 2006; 2006; 12(13): 3890–5. [PubMed: 16818683]

29. Wang H, Lindsey S, Konieczna I, Bei L, Horvath E, Huang W. Constitutively active SHP2 cooperates with HoxA10 overexpression to induce acute myeloid leukemia. J Biol Chem. 2009; 284:2549–2567. [PubMed: 19022774]

30. Zhou X, Coad J, Ducatman B, Agazie YM. SHP2 is up-regulated in breast cancer cells and in infiltrating ductal carcinoma of the breast, implying its involvement in breast oncogenesis. Histopathology. 2008; 53:389–402. [PubMed: 18643929]

31. Mohi MG, Neel BG. The role of Shp2 (PTPN11) in cancer. Curr Opin Genet Dev. 2007; 17:23–30. [PubMed: 17227708]

32. Niu J, Huang YJ, Wang LE, Sturgis EM, Wei Q. Genetic polymorphisms in the PTPN13 gene and risk of squamous cell carcinoma of head and neck. Carcinogenesis. 2009; 30:2053–2058. [PubMed: 19892796]

33. Mita Y, Yasuda Y, Sakai A, Yamamoto H, Toyooka S, Gunduz M, et al. Missense polymorphisms of PTPRJ and PTPN13 genes affect susceptibility to a variety of human cancers. J Cancer Res Clin Oncol. 2010; 136:249–259. [PubMed: 19672627]

34. Warabi M, Nemoto T, Ohashi K, Kitagawa M, Hirokawa K. Expression of protein tyrosine phosphatases and its significance in esophageal cancer. Exp Mol Pathol. 2000; 68:187–195. [PubMed: 10816386]

35. Zatelli MC, Piccin D, Tagliati F, Bottoni A, Luchin A, degli Uberti EC. SRC homology-2-containing protein tyrosine phosphatase-1 restrains cell proliferation in human medullary thyroid carcinoma. Endocrinology. 2005; 146:2692–2698. [PubMed: 15746253]

36. Fujita M, Zhu X, Sasaki K, Ueda R, Low KL, Pollack IF, Okada H. Inhibition of STAT3 promotes the efficacy of adoptive transfer therapy using type-1 CTLs by modulation of the immunological microenvironment in a murine intracranial glioma. J Immunol. 2008; 180:2089–2098. [PubMed: 18250414]

37. Ogino T, Bandoh N, Hayashi T, Miyokawa N, Harabuchi Y, Ferrone S. Association of tapasin and HLA class I antigen down-regulation in primary maxillary sinus squamous cell carcinoma lesions with reduced survival of patients. Clin Cancer Res. 2003; 9:4043–4051. [PubMed: 14519625]

38. Matsui M, Ikeda M, Akatsuka T. High expression of HLA-A2 on an oral squamous cell carcinoma with down-regulated transporter for antigen presentation. Biochem Biophys Res Commun. 2001; 280:1008–1014. [PubMed: 11162627]

39. Seliger B, Atkins D, Bock M, Ritz U, Ferrone S, Huber C, et al. Characterization of human lymphocyte antigen class I antigen-processing machinery defects in renal cell carcinoma lesions with special emphasis on transporter-associated with antigen-processing down-regulation. Clin Cancer Res. 2003; 9:1721–1727. [PubMed: 12738726]

40. Atkins D, Breuckmann A, Schmahl GE, Binner P, Ferrone S, Krummenauer F, et al. MHC class I antigen processing pathway defects, ras mutations and disease stage in colorectal carcinoma. Int J Cancer. 2004; 109:265–273. [PubMed: 14750179]

41. Restifo NP, Esquivel F, Kawakami Y, Yewdell JW, Mule JJ, Rosenberg SA, et al. Identification of human cancers deficient in antigen processing. J Exp Med. 1993; 177:265–272. [PubMed: 8426105]

42. Seliger B, Ritz U, Abele R, Bock M, Tampe R, Sutter G, et al. Immune escape of melanoma: first evidence of structural alterations in two distinct components of the MHC class I antigen processing pathway. Cancer Res. 2001; 61:8647–8650. [PubMed: 11751378]

43. Haspel RL, Darnell JE Jr. A nuclear protein tyrosine phosphatase is required for the inactivation of Stat1. Proc Natl Acad Sci USA. 1999; 96:10188–10193. [PubMed: 10468584]

44. Chan RJ, Feng GS. PTPN11 is the first identified proto-oncogene that encodes a tyrosine phosphatase. Blood. 2007; 109:862–867. [PubMed: 17053061]

45. Lapteva N, Huang XF. CCL5 as an adjuvant for cancer immunotherapy. Expert Opin Biol Ther. 2010; 10:725–733. [PubMed: 20233026]

46. Sallusto F, Lenig D, Mackay CR, Lanzavecchia A. Flexible programs of chemokine receptor expression on human polarized T helper 1 and 2 lymphocytes. J Exp Med. 1998; 187:875–883. [PubMed: 9500790]

47. Lavergne E, Combadiere C, Iga M, Boissonnas A, Bonduelle O, Maho M, et al. Intratumoral CC chemokine ligand 5 overexpression delays tumor growth and increases tumor cell infiltration. J Immunol. 2004; 173:3755–3762. [PubMed: 15356122]

48. Addison CL, Arenberg DA, Morris SB, Xue YY, Burdick MD, Mulligan MS, et al. The CXC chemokine, monokine induced by interferon-gamma, inhibits non-small cell lung carcinoma tumor growth and metastasis. Hum Gene Ther. 2000; 11:247–261. [PubMed: 10680839]

49. Harlin H, Meng Y, Peterson AC, Zha Y, Tretiakova M, Slingluff C, et al. Chemokine expression in melanoma metastases associated with CD8+ T-cell recruitment. Cancer Res. 2009; 69:3077–3085. [PubMed: 19293190]
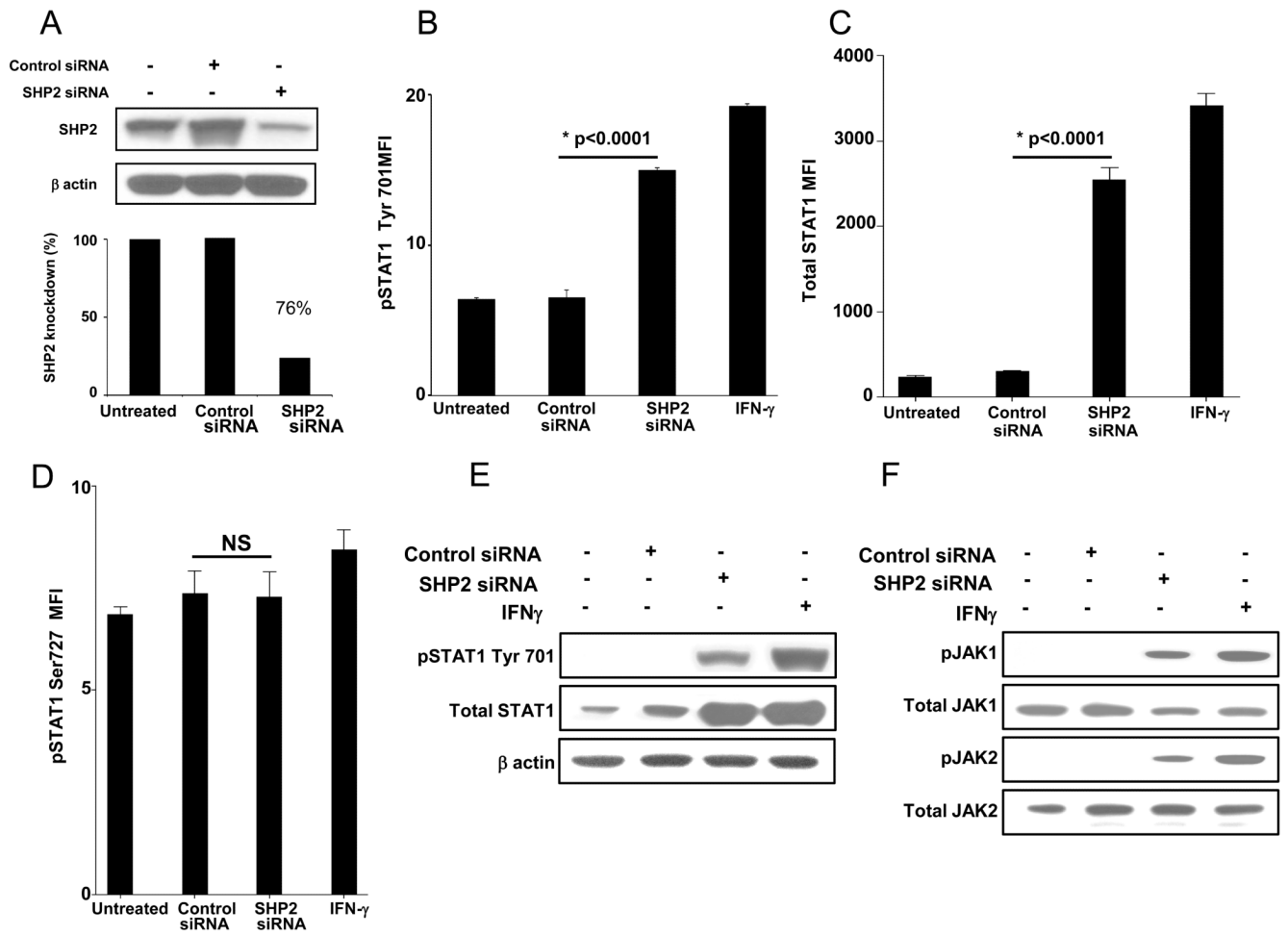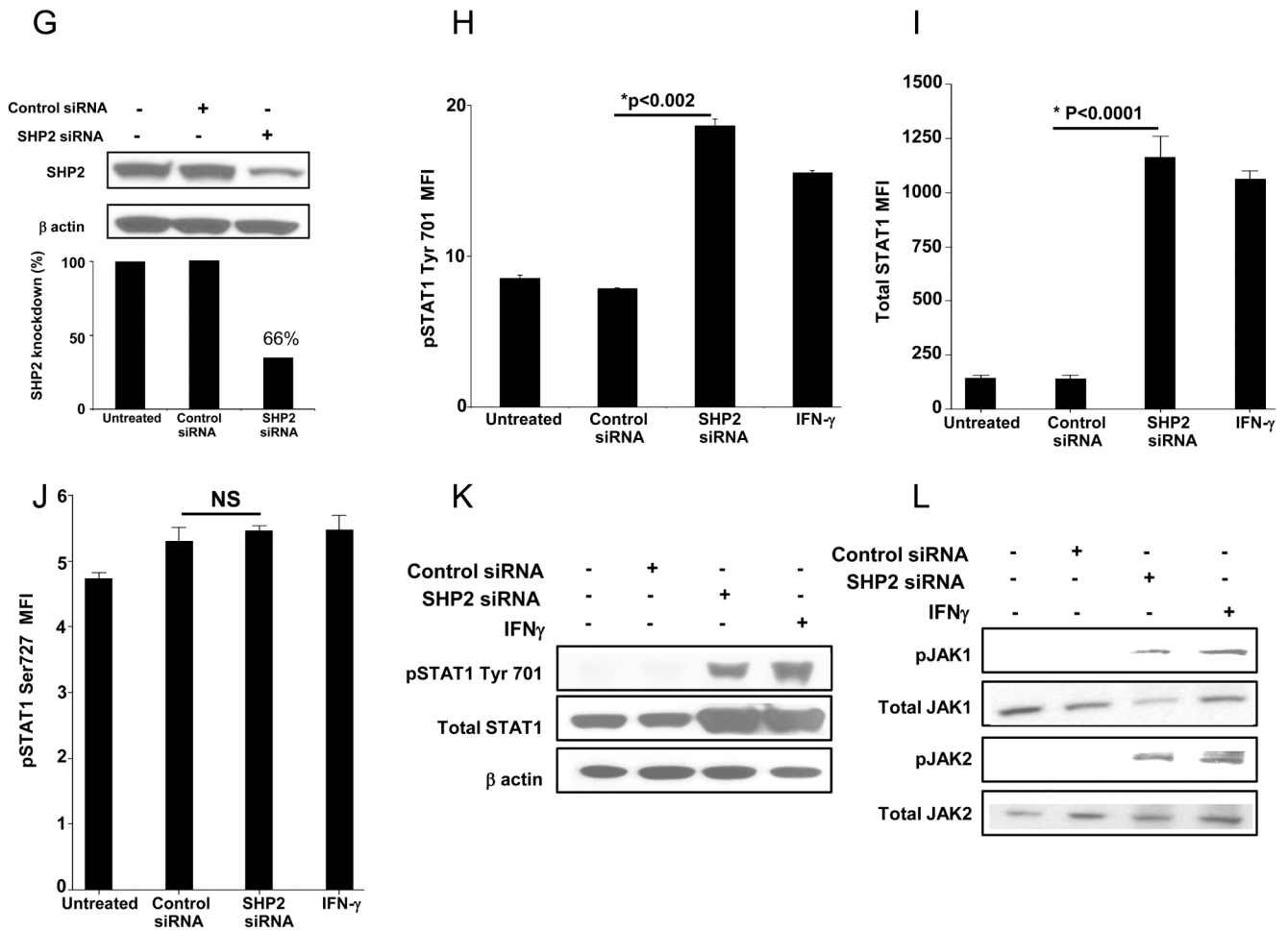
Translational Relevance

T cell-based cancer immunotherapy is an encouraging area of investigation with emerging clinical efficacy. The failure to address the tumor as a defective target for T cell recognition has been a major obstacle to its success. Here, we report a novel therapeutic target in head and neck cancer (HNC) that alters the immunogenicity of the tumor. Src homology-2 domain-containing phosphatase (SHP2) was found to be overexpressed in HNC, which when depleted, restored recognition of HNC cells by cytotoxic T lymphocytes and induced secretion of pro-inflammatory, T cell attracting chemokines, RANTES and IP10. These findings provide the rationale for future investigation of the effects of small molecule SHP2 inhibitors on tumor growth *in vivo*, functioning as a potential adjuvant to enhance T cell-based immunotherapy of cancer.
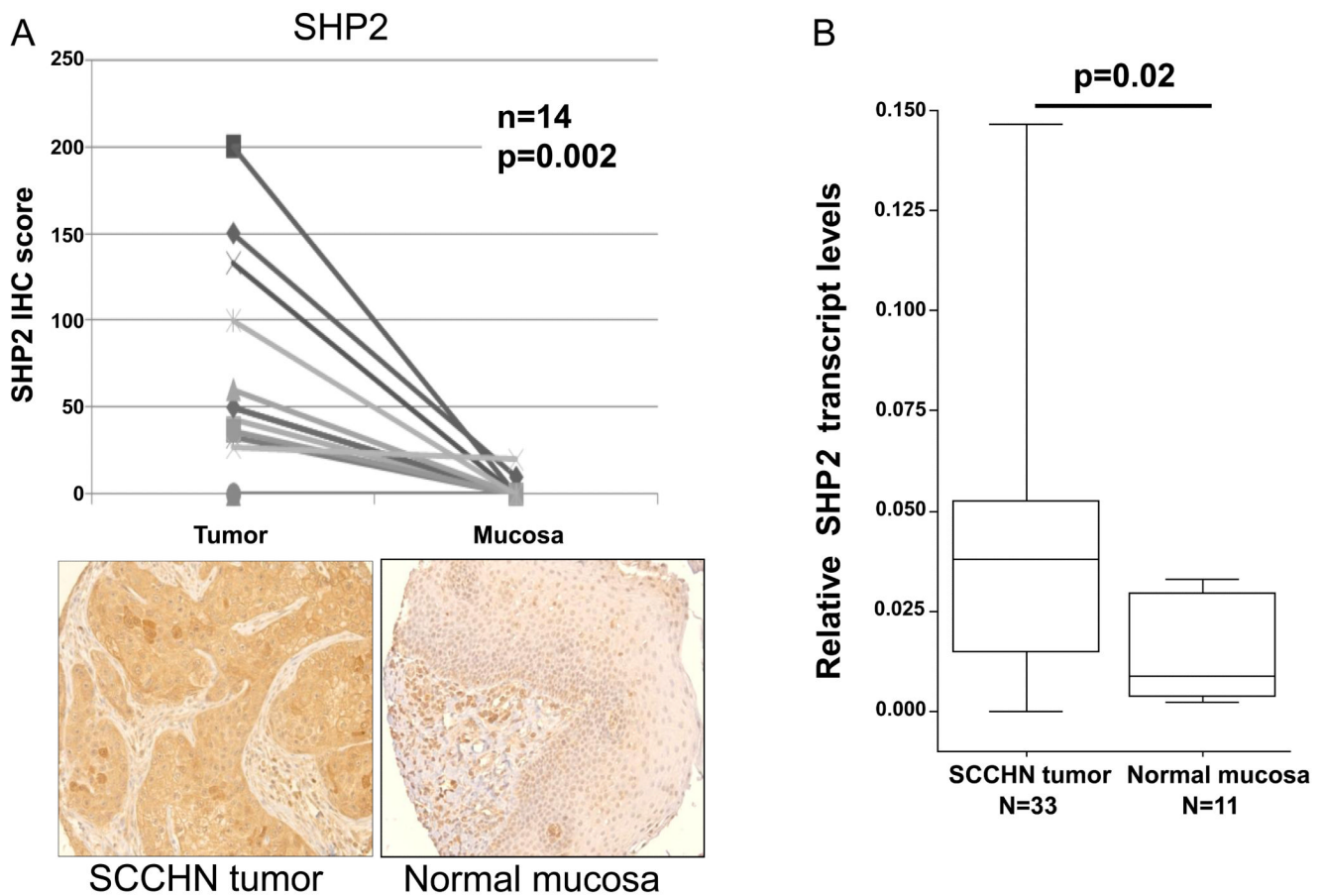
Figure 1. SHP2 is overexpressed in HNC tissue but not in normal mucosa
(A) HNC tumors and normal adjacent mucosa were stained with an anti-SHP2 mAb (as described in "Materials and Methods"). The IHC semi-quantitative score was derived by two independent pathologists, by multiplying the staining intensity (scored as $0 - 3$) by the percent of tumor cells stained (0-100%), to the nearest 5%. IHC scores for each core of a specimen were averaged (n=14) and statistically analyzed. Representative examples at 200x magnification of SHP2 from HNC tissue and normal mucosa are provided. (B) cDNA from HNC tumors (n=33) and normal adjacent mucosa (n=11) were subjected to quantitative real time PCR analysis (as described in materials and methods). Relative expression of shp2 transcript to endogenous control gene (β-actin) was calculated using the ΔC_T method: relative expression = $2^{-\Delta C_T}$, where $\Delta C_T = C_{T\ (shp2)} - C_{T\ (\beta\text{-actin})}$. Two-tailed unpaired t-test was performed for statistical analysis.

A

Control siRNA − + −
SHP2 siRNA − − +

SHP2

β actin

SHP2 knockdown (%)

100

50

76%

Untreated | Control siRNA | SHP2 siRNA

B

pSTAT1 Tyr 701MFI

20

* p<0.0001

10

0

Untreated | Control siRNA | SHP2 siRNA | IFN-γ

C

Total STAT1 MFI

4000

3000

2000

1000

* p<0.0001

Untreated | Control siRNA | SHP2 siRNA | IFN-γ

D

pSTAT1 Ser727 MFI

10

NS

5

0

Untreated | Control siRNA | SHP2 siRNA | IFN-γ

E

Control siRNA − + − −
SHP2 siRNA − − + −
IFNγ − − − +

pSTAT1 Tyr 701

Total STAT1

β actin

F

Control siRNA − + − −
SHP2 siRNA − − + −
IFNγ − − − +

pJAK1

Total JAK1

pJAK2

Total JAK2

**Figure 2. SHP2 depletion upregulates pSTAT1, pJAK-1/2 and total STAT1**
(A-F) PCI-13 and (G-L) SCC-90 cells were transfected with SHP2 siRNA (100 nM, 48 hr)
which significantly reduced SHP2 expression in HNC cells by western blot analyses. SHP2
depletion also significantly upregulated pSTAT1 and its target gene product STAT1 as
determined by intracellular flow cytometry and immunblotting compared to control siRNA
in (B, C, E) PCI-13 and (H, I, K) SCC-90 cells. SHP2 depletion also upregulated pJAK1
(Tyr1022/1023) and pJAK2 (Tyr 1007/1008) compared to control siRNA in (F) PCI-13 and
(L) SCC-90 cells. The cells were treated with IFN-γ (100 U/ml=1464 pg/ml, 48h) as a
positive control for STAT1 phosphorylation. Data represent three independent experiments
and error bars indicate standard error.
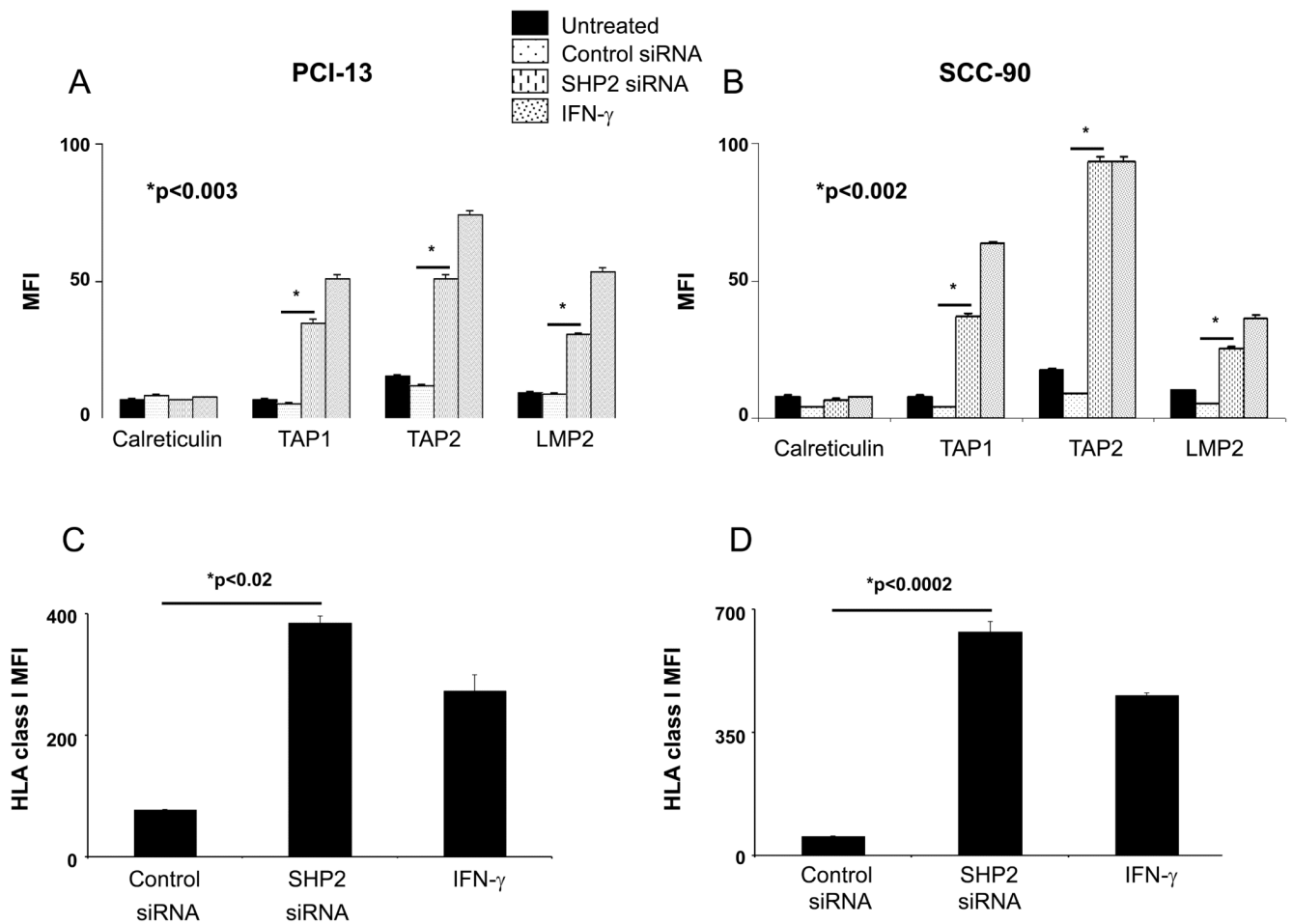
Figure 3. SHP2 depletion upregulates HLA class I APM components

PCI-13 and SCC-90 cells were untreated, treated with IFN-γ (100 U/ml=1464 pg/ml, 48 hr), transfected with control siRNA (100 nM, 48 h) or SHP2 siRNA (100 nM, 48 hr). Flow cytometric analyses of intracellular stained cells for TAP1, TAP2, and LMP2 APM components in (A) PCI-13 and (B) SCC-90 cells. Calreticulin, a non-IFN-γ inducible APM component was included to control for global changes in protein expression following transfection. Mean fluorescence intensity (MFI) was measured and error bars indicate standard error. Data represent three independent experiments and error bars indicate standard error. (C) PCI-13 and (D) SCC-90 cells were treated as described above, and HLA class I expression was measured by flow cytometeric MFI. Data represent three independent experiments and error bars indicate standard error.
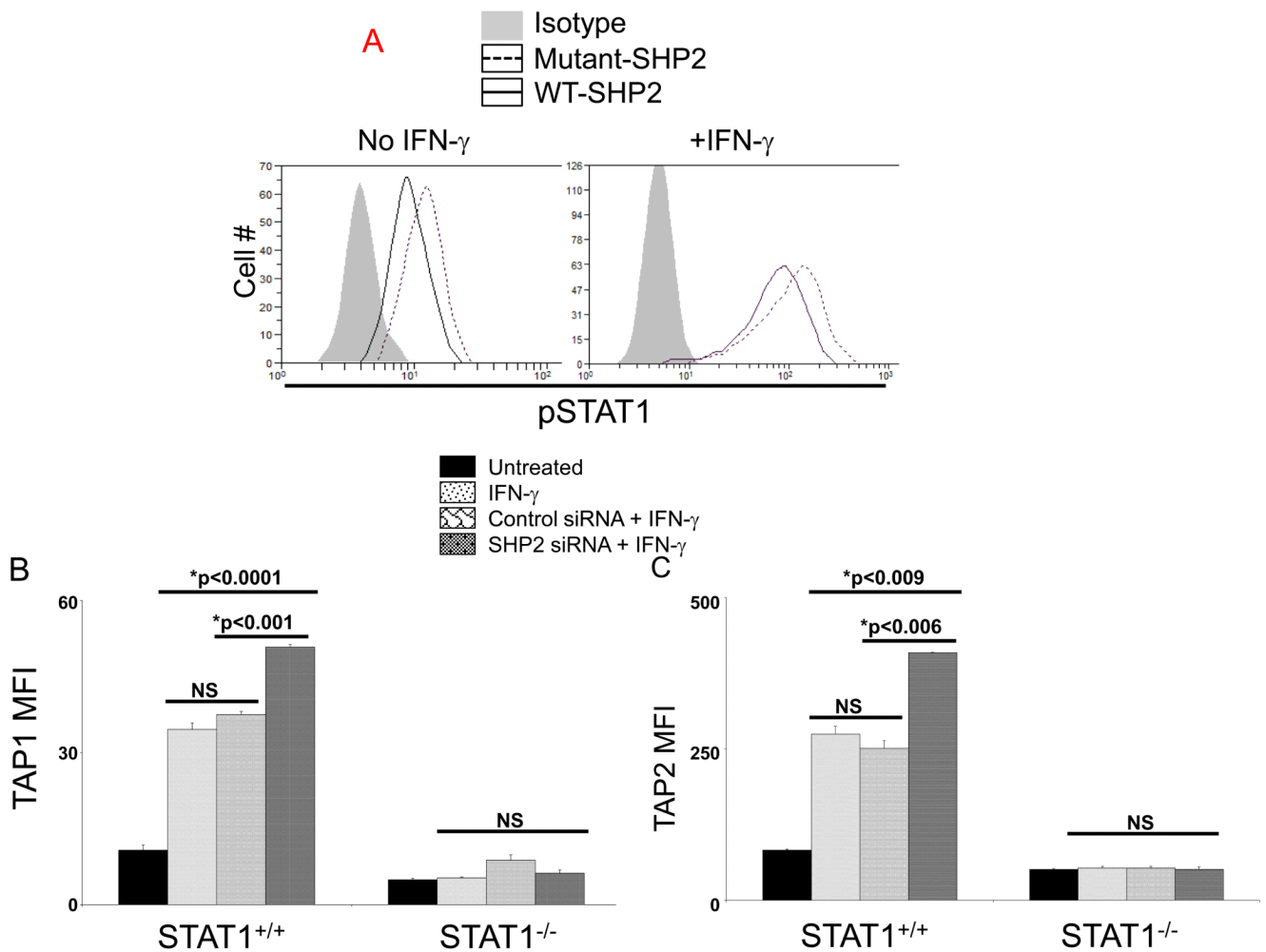
Figure 4. SHP2 decreases basal and IFN-γ induced pSTAT1 and TAP1/2 expression
(A) Keratinocytes transfected with wild-type SHP2 decreased basal and IFN-γ (10 U/ml=146.4pg/ml, 30 min) induced pSTAT1 compared to mutant SHP2. (C) Parental 2fTGH (STAT1$^{+/+}$) and U3A (STAT1$^{-/-}$) fibrosarcoma cells were treated with IFN-γ (10 U/ml=146.4 pg/ml) for 48 hr alone or 24 hours after transfection with SHP2 (50 nM) or control siRNA. Flow cytometric analyses were used to determine TAP1 and TAP2 expression and the data were plotted by MFI. Data represent three independent experiments and error bars indicate standard error.
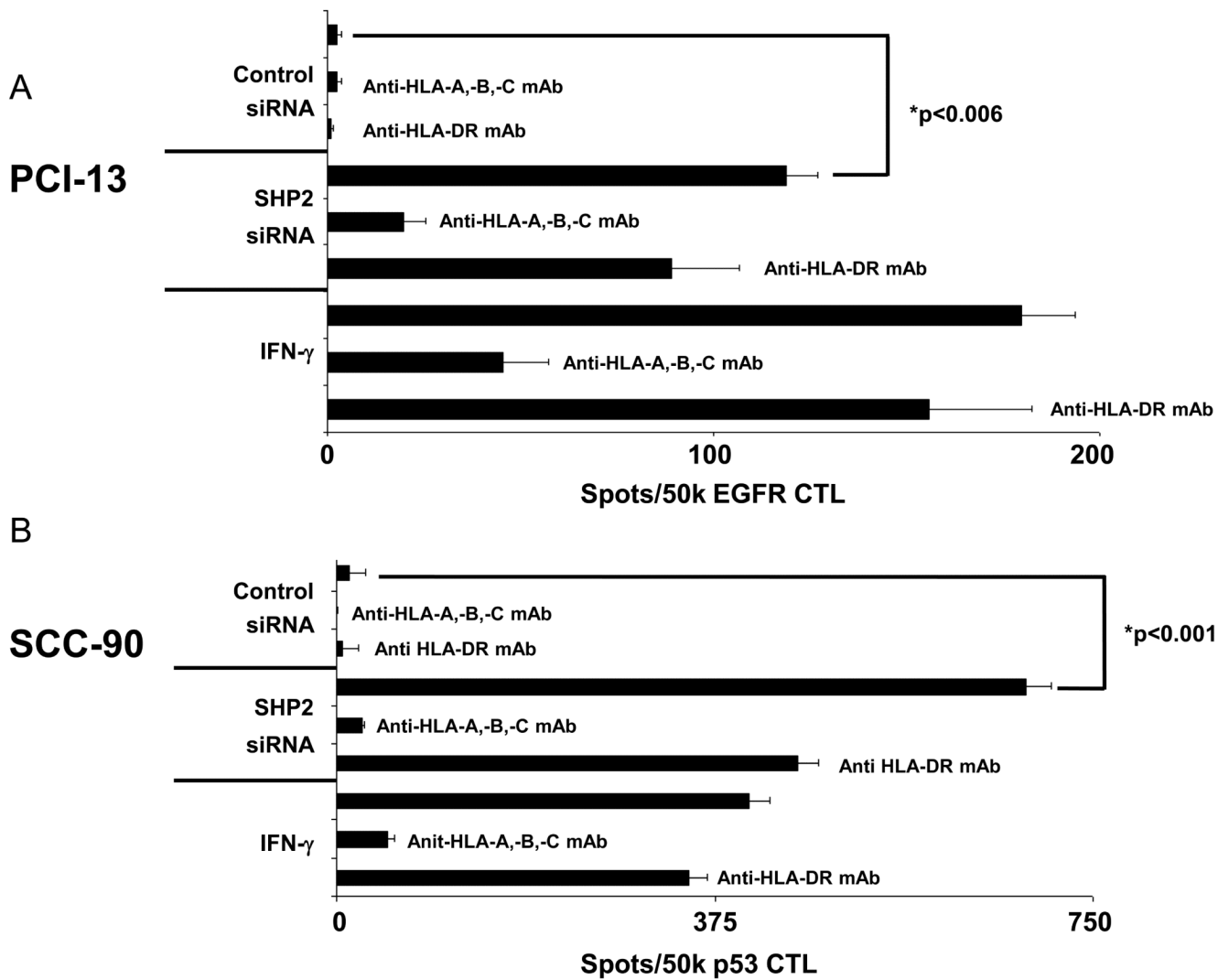
Figure 5. SHP2 knockdown restores HNC cell recognition by TA-specific CTL
IFN-γ ELISPOT assays were performed to detect recognition by TA-specific CTL of (A)
PCI-13 and (B) SCC-90 cells following SHP2 knockdown. Cells were untreated, treated
with IFN-γ (100 U/ml=1464 pg/ml, 48 hr), control siRNA (100 nM, 48 hr) or SHP2 siRNA
(100 nM, 48 hr). EGFR$_{853-861}$ and p53$_{65-73}$ specific cytotoxic T lymphocytes (CTL) were
used as effector cells. The HLA class I-specific mAb W6/32 and the HLA-DR-specific mAb
L243 were used to demonstrate that the recognition of target cells by TA-specific CTL was
HLA class I restricted. Data represent a single experiment performed in triplicate and error
bars indicate standard error.
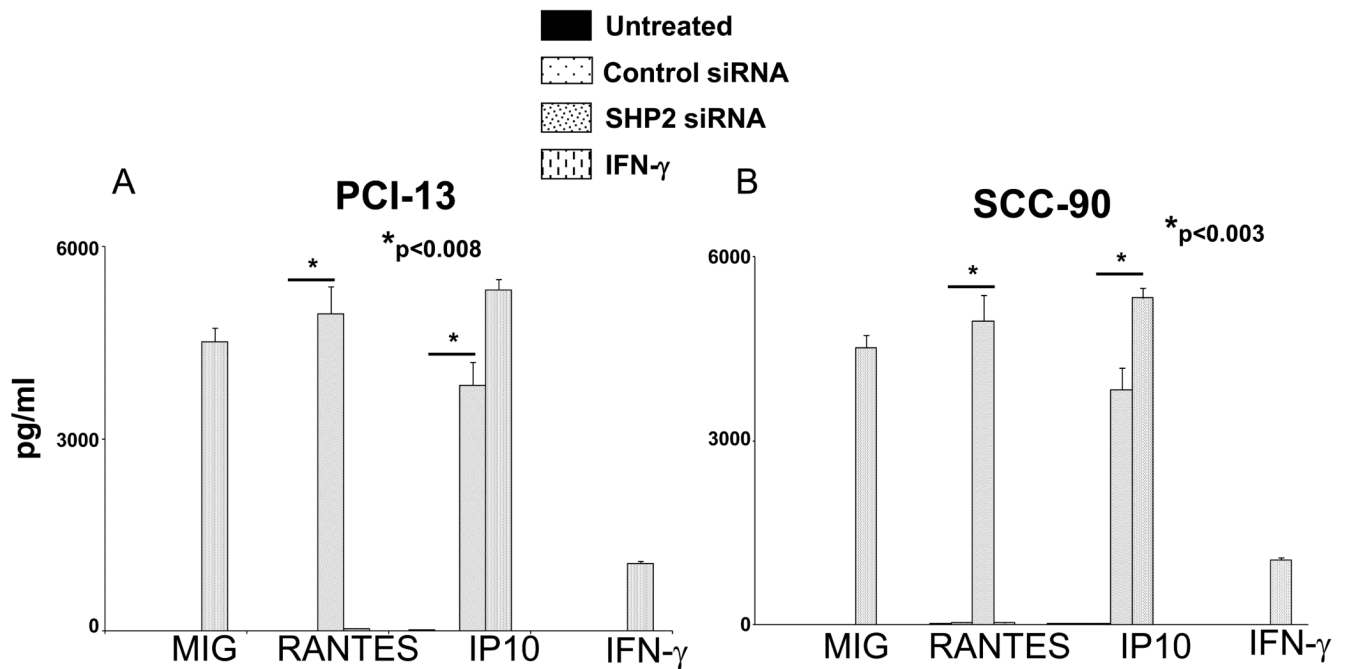
Figure 6. SHP2 siRNA induced the secretion of RANTES and IP10 from HNC cells
Multiplex ELISA (Luminex™) assays were performed on supernatants from (A) PCI-13 and
(B) SCC-90 cells following transfection with the indicated siRNA (100 nM, 48 hr) or
treatment with IFN-γ (100 U/ml=1464 pg/ml, 48 hr). Data represent three independent
experiments and error bars indicate standard error.